

# KrF excimer laser-fabricated Bragg grating in optical microfiber made from pre-etched conventional photosensitive fiber

Zhengtong Wei (卫正统), Nuan Jiang (姜 暖), Zhangqi Song (宋章启)\*,  
Xueliang Zhang (张学亮), and Zhou Meng (孟 洲)

*College of Optoelectronic Science and Engineering, National University of Defense Technology,  
Changsha 410073, China*

\*Corresponding author: songzhangqi@nudt.edu.cn

Received October 24, 2012; accepted December 7, 2012; posted online March 28, 2013

A method to fabricate fiber Bragg grating (FBG) in an optical microfiber (OM) from a conventional photosensitive fiber is proposed in this letter. The cladding of a conventional photosensitive fiber is etched to 17  $\mu\text{m}$ . The etched fiber is drawn to an OM 6  $\mu\text{m}$  in diameter. The photosensitivity of the fabricated OM is effectively reserved. A FBG in the OM (MFBG) is successfully fabricated using a KrF excimer laser at a fluence of 400  $\text{mJ}/\text{cm}^2$  through a phase mask with a pitch of 1089.3 nm. The reflectivity of the FBG is approximately 10%, and the 3-dB spectrum bandwidth is 0.13 nm. The concentration of brine is measured by immersing the MFBG in the liquid, and the minimum detectable refractive index variation can reach  $7.2 \times 10^{-5}$  at a refractive index value of 1.33.

OCIS codes: 060.3738, 060.2370, 230.4000.

doi: 10.3788/COL201311.040603.

Recently, optical microfibers (OMs) have attracted considerable attention because of the vast progress in the fabrication of low-loss structures that allow for low-loss evanescent waveguiding<sup>[1–4]</sup>. OMs have numerous advantages in the field of fiber optic sensing because of their outstanding optical properties, including large evanescent field, small effective mode field diameter, high non-linearity, and convenient connectivity to other fiberized components. So far, OMs have been successfully studied in sensing humidity<sup>[5]</sup>, refractive index<sup>[6]</sup>, temperature<sup>[7]</sup>, gas concentration<sup>[8]</sup>, and current<sup>[9]</sup>. Light transmission in OMs is confined tightly to the core region because of the large contrast in the refractive index between OMs and air, whereas a relatively large fraction of the guided power propagates out of the physical boundary as the evanescent field, which makes it highly sensitive to the tested medium.

In recent years, fiber Bragg grating (FBG) has been utilized widely in the field of fiber optic sensing. However, it is not sensitive to the refractive index of the surrounding medium. In general, this problem can be solved using two methods. One is etching the fiber after FBG creation, and the other is fabricating a long-period fiber grating (LPFG). The mechanical strength of the etched fiber is greatly reduced, which limits the applications of FBG-based refractive index sensors<sup>[10]</sup>. LPFG possesses a broad bandwidth transmission dip, which makes it unsuitable for sensor multiplexing. Moreover, bending has a cross-sensitivity issue<sup>[11]</sup>. FBG written in an OM (MFBG) is proposed to sense the refractive index<sup>[12]</sup>. Recently, femtosecond laser pulses<sup>[13]</sup>, CO<sub>2</sub> lasers<sup>[14]</sup>, focused ion beam technology<sup>[15–18]</sup>, and ArF excimer laser<sup>[19,20]</sup> have been used to fabricate MFBG. Gratings in Refs. [13,14] were inscribed using high-intensity laser pulses to cause physical deformation on OMs. References [19,20] revealed that the key challenge in using ArF excimer lasers was overcoming the large at-

tenuation of the writing beam by scattering the lattice structure<sup>[21]</sup>. In this letter, a KrF excimer laser was used to write FBG in an OM, which was more popular in the commercial fabrication of FBG.

Fiber photosensitivity is related to the concentration of Ge. However, Ge is only doped in the core of a conventional photosensitive fiber. When it is tapered to an OM, its photosensitivity is highly reduced because of the dispersion of Ge. To fabricate MFBG, an OM with high photosensitivity is needed. A previous study used a Ge/B-codoped photosensitive fiber to fabricate MFBG using a KrF excimer laser<sup>[22]</sup>. However, its fabrication is expensive and difficult<sup>[19]</sup>.

In this letter, we propose a two-step method to fabricate a photosensitive OM with a conventional photosensitive fiber. Firstly, most cladding for a conventional photosensitive fiber is etched with HF acid, whereas the core doped with Ge is kept. Secondly, the etched fiber is drawn to the OM using a modified flame-brush method<sup>[1]</sup>. Compared with the OM drawn directly from conventional fibers without etching, the etch-and-taper method can improve the concentration of Ge and enhance the photosensitivity of the OM. Then, FBG is written in the OM with a KrF excimer laser, and the fabricated MFBG is used to sense the concentration of the brine.

The photosensitivity of the OM can be effectively reserved by first reducing the cladding, making the fabrication of MFBG using a conventional photosensitive optical fiber simple. Furthermore, when the etched fiber is equally drawn to the OM by heating, the unevenness of the profile can be smoothed and the mechanical strength can be suitably improved.

When the MFBG is used in refractive index sensing, the OM can be assumed to have a circular cross-section, an infinite cladding, a step-index profile, and single-mode propagation. Briefly, the single-mode condition of a step-index waveguide can be described as

$V = 2\pi a \sqrt{n_1^2 - n_2^2} / \lambda \leq 2.405$ , where  $a$  is the radius of the OM,  $\lambda$  is the optical wavelength in a vacuum, and  $n_1$  and  $n_2$  denote the refractive indices of the core and the cladding, respectively. In this experiment,  $n_1$  is approximately 1.45 (refractive index of core),  $n_2$  is approximately 1.33 (refractive index of water), and  $\lambda$  is 1.55  $\mu\text{m}$ . In our case,  $a$  is 3  $\mu\text{m}$ , which means that tens of higher-order modes besides the fundamental mode can be supported in the OM. According to coupled-mode theory at the phase-matching condition<sup>[23]</sup>, the effective modal indices of the incident wave and grating-coupled reflected wave are the same for the condition considered in this letter. Hence, a coherent exchange wavelength between the modes is given as

$$\lambda_{\text{MFBG}} = 2n_{\text{eff}}\Lambda_{\text{MFBG}}, \quad (1)$$

where  $\lambda_{\text{MFBG}}$  is the reflected wavelength,  $\Lambda_{\text{MFBG}}$  is the grating period, and  $n_{\text{eff}}$  is the effective modal index transmitted in the OM.

Effective mode coupling depends on the overlaps among the forward-guiding mode field distribution, the backward-guiding mode field distribution, and the cross-sectional shape of the MFBG. For the different field distributions of various modes in the OM, only some modes have sufficient field overlaps in the grating region. Therefore, these modes can couple effectively, whereas other modes hardly have any effective overlap in the grating region of an OM, causing the coupling coefficients of these modes to approach zero<sup>[22]</sup>. For the OM of 6  $\mu\text{m}$  in diameter, only modes  $\text{HE}_{11}$  and  $\text{HE}_{12}$  can effectively couple to the backward guiding (reflected wavelength). In this letter, we only considered the reflection of the fundamental mode. The higher-order mode is attenuated by bending the single-mode fiber with small radius, and the taper length is set to be sufficiently long to avoid any mode conversion<sup>[24]</sup>.

The effective modal index of the fundamental mode ( $n_{\text{eff}}$ ) in the OM with different diameters can be numerically calculated according to the eigenvalue equations solved from Maxwell's equations<sup>[25]</sup>. When the refractive index of the surrounding medium changes, the effective modal index transmitted in the OM changes accordingly, and the reflected wavelength of MFBG shifts according to Eq. (1). The shift of the reflected wavelength ( $\Delta\lambda_{\text{MFBG}}$ ) divided by the change in ambient refractive index ( $\Delta n$ ) is the refractive index sensitivity ( $K_n$ ) of the MFBG. According to Eq. (1), the reflected wavelength  $\lambda_{\text{MFBG}}$  is related only to  $n_{\text{eff}}$  and  $\Lambda_{\text{MFBG}}$  (half of the phase mask pitch). Therefore, we can obtain  $K_n$  as

$$K_n = \frac{\Delta\lambda_{\text{MFBG}}}{\Delta n} = \frac{2\Delta n_{\text{eff}}\Lambda_{\text{MFBG}}}{\Delta n}. \quad (2)$$

The refractive index sensitivity of the MFBG with different diameters can be calculated according to Eq. (2). As shown in Fig. 1, the sensitivity varies with a change in ambient refractive index. More energy propagates outside the fiber for the OM with thinner diameter, thus exhibiting a higher sensitivity to the ambient refractive index. For the fundamental mode of the OM 6  $\mu\text{m}$  in diameter, the refractive index sensitivity obtained is 13.7 nm per refractive index unit (RIU) at a surrounding refractive index value of 1.33.

Normally, Ge is mainly doped in the core of a conventional photosensitive optical fiber. Ge disperses to the outer cladding if a section of a normal photosensitive optical fiber is tapered onto an OM. For the OM (6  $\mu\text{m}$  in diameter) directly drawn from a normal photosensitive fiber with 125- $\mu\text{m}$  cladding, the average concentration of Ge declines to approximately one four-hundredth of the original fiber. Therefore, writing FBG in it will be very difficult.

In this letter, a conventional photosensitive fiber with a Ge-doped core 6  $\mu\text{m}$  in diameter was used, and a 125- $\mu\text{m}$  cladding was first etched to a diameter of 17  $\mu\text{m}$  using HF acid. Then, the etched fiber was drawn to an OM 6  $\mu\text{m}$  in diameter using an OM manufacturing system. The schematic illustration of the progress is shown in Figs. 2(a) and (b). In our experiment, the relative rate of the hot-zone change and taper elongation is 0.1<sup>[26]</sup>, the taper length is 6.5 mm, and the OM waist length is 15 mm. Hence, the OM structure in our experiment is adiabatic<sup>[24]</sup>. The additional loss for the OM is approximately 0.5 dB. After heating and drawing, the Ge doped in the core disperses to the outer cladding. The diameter of the core doped with Ge is approximately 6  $\mu\text{m}$  for the etched fiber of 17  $\mu\text{m}$  in diameter. Hence, if the Ge doped in the core diffuses to the whole region of the OM, the concentration of Ge decreases to approximately one-eighth of the initial one, which increases by approximately 50 times than that of the directly drawn OM.

Compared with the method without etching, the two-step method for fabricating OM improves the concentration of Ge in the OM effectively. However, the photosensitivity of the OM is still reduced compared with that of the initially used photosensitive fiber. To increase its photosensitivity further, the fabricated OM was loaded with hydrogen at a pressure of 2000 psi for 200 h at room temperature. After hydrogen loading, the OM was cleaned with alcohol. The insertion loss of the hydrogen-loaded OM was approximately 1.5 dB higher than that of the initial OM.

In the fabrication of MFBG, we used a 248-nm KrF-excimer laser with a repetition rate of 10 Hz and a fluence of approximately 400  $\text{mJ}/\text{cm}^2$  through a 12-mm-long phase mask with a pitch of 1089.3 nm. The MFBG was formed after approximately 120 pulses of irradiation, and the schematic illustration is shown in Fig. 2(c).

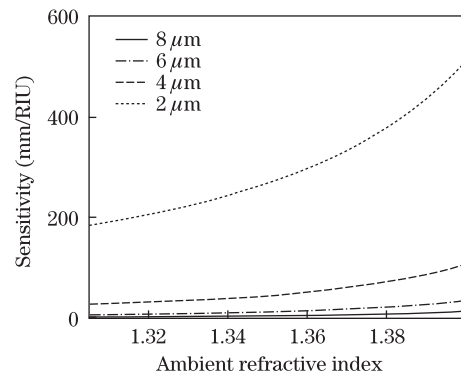


Fig. 1. Refractive index sensitivity versus different ambient refractive indices for different diameters of OM.

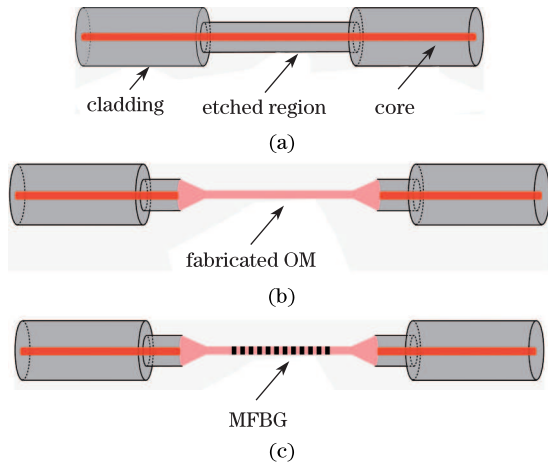


Fig. 2. Schematic illustration of the MFBG fabrication process. (a) A conventional photosensitive fiber is etched using HF acid, (b) the etched fiber is drawn to OM, and (c) the fabricated OM is loaded with hydrogen and the MFBG is formed with a 248-nm KrF-excimer laser.

The reflection and the transmission spectra of the fabricated MFBG are shown in Fig. 3. The reflection spectrum of the MFBG was tested by an optical sensing interrogator (SM125 from MOI Company) with an accuracy of 1 pm, and the normalized intensity of the transmission spectrum was measured with an amplified spontaneous emission source and an optical spectrum analyzer with an accuracy of 0.01 nm. The peak reflected wavelength in Fig. 3(a) is 1565.845 nm, and the peak transmitted wavelength in Fig. 3(b) is 1565.85 nm. The reflectivity of the MFBG is approximately 10%, and the 3-dB spectrum bandwidth of the MFBG is approximately 0.13 nm. During fabrication, a part of the laser may focus on the conical region of the OM, which may have caused the asymmetry of the spectra shown in Fig. 3.

In our experiments, the grating period is 544.65 nm, and the effective modal index of the fundamental mode in the OM 6  $\mu\text{m}$  in diameter is 1.4375. According to Eq. (1), the reflected wavelength for the MFBG is approximately 1565.6 nm, which is almost the same with the experimental result.

To obtain higher sensitivity, an OM with thinner diameter is needed. This OM with thinner diameter can cause more fraction of power to be transmitted out of the physical boundary, which may lead to a decrease in reflectivity. In addition, the 3-dB spectrum bandwidth may broaden because of the larger waveguide dispersion.

The experiment was designed to demonstrate the feasibility of the MFBG for refractive index sensing. The reflected spectrum of the sensing OM was measured by an optical sensing interrogator. When the MFBG is immersed in pure water from a commercial purification system, a red shift of the reflection peak is observed accordingly (Fig. 4(a)). When the MFBG is immersed in absolute ethyl alcohol, a further red shift of the reflection peak is observed (Fig. 4(a)).

Given that the refractive index of alcohol is larger than that of pure water, the reflected wavelength in alcohol is longer than that in pure water. The reflected wavelength as a function of the ambient refractive index-

dex is numerically solved according to Eq. (1) with  $\Lambda_{\text{MFBG}} = 544.65$  nm,  $n_1 = 1.451$ , and  $a = 3$   $\mu\text{m}$ . The experimental and numerical calculation results are plotted in Fig. 4(b), showing that the reflected wavelengths extracted from the experimental results agree well with the numerical calculation.

Compared with the normal FBG, MFBG is potentially more sensitive to the change in the outer refractive index. A concentration-sensing experiment was performed by immersing the MFBG in brine solutions with different concentrations at room temperature. The reflected wavelengths of the sensing MFBG corresponding to different concentrations of the designed brine are obtained and plotted in Fig. 5. The linear fitting data are also plotted in line. We calculated the corresponding refractive index of brine (Fig. 5). According to Ref. [27], the refractive index variation is approximately 0.0079 for the change

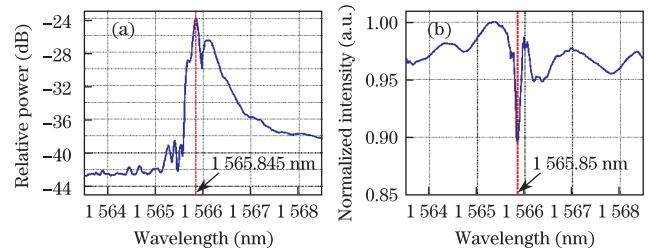


Fig. 3. (a) Reflection spectrum of the MFBG tested using an optical sensing interrogator; (b) normalized intensity of the transmission spectrum measured by an optical spectrum analyzer.

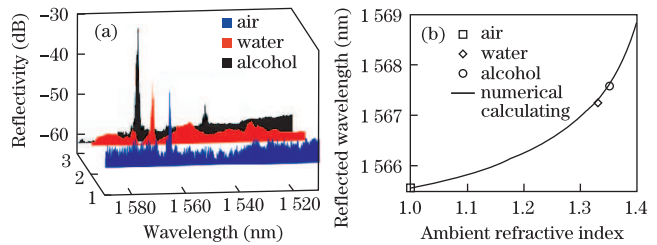


Fig. 4. (a) Reflected spectra of the MFBG in air ( $n_2 = 1$ ), water ( $n_2 = 1.33$ ), and alcohol ( $n_2 = 1.36$ ); (b) reflected wavelength as a function of the refractive index of ambient material, and the markers are reflected wavelengths extracted from (a). The numerical fitting curve is calculated using Eq. (1) with parameters  $n_1 = 1.451$  and  $a = 3$   $\mu\text{m}$ .

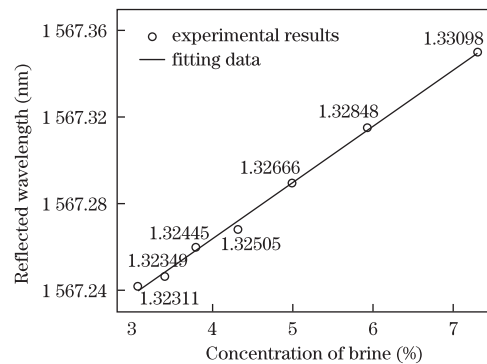


Fig. 5. Reflected wavelengths of the MFBG corresponding to different concentrations of brine. The refractive indices of brine are labeled near each measured data.

in the concentration of brine from 3.05% to 7.30%, which agrees well with the estimated results. As shown in Fig. 5, the wavelength shift is approximately 0.11 nm. Hence, the refractive index sensitivity of the MFBG is approximately 13.9 nm/RIU at a refractive index value of 1.33, which is in good agreement with the simulation result. Considering that the accuracy of the optical sensing interrogator is 1 pm, the minimum detectable refractive index variation can reach  $7.2 \times 10^{-5}$ .

In conclusion, a MFBG is successfully fabricated with a KrF excimer laser using an OM made from a pre-etched conventional photosensitive fiber. The two-step method can fabricate an OM with a relatively higher photosensitivity than the OM tapered directly from a photosensitive fiber of 125  $\mu\text{m}$  in diameter. The reflectivity of the MFBG is approximately 10%, and the 3-dB spectrum bandwidth of the MFBG is 0.13 nm. The reflected wavelength in the experiment is in accordance with the simulated result. The concentration of brine was measured by immersing the MFBG in the liquid with a sensitivity of 13.9 nm/RIU at a refractive index value of 1.33. The minimum refractive index variation that can be detected is  $7.2 \times 10^{-5}$ . In future works, higher sensitivity of the MFBG can be obtained using thinner OM, and the control of the profile in tapering the etched fiber should be more accurate to prevent the irregularity of the reflected wavelength.

## References

1. G. Brambilla, *J. Opt.* **12**, 043001 (2010).
2. M. Sumetsky, *Opt. Express* **12**, 2303 (2004).
3. F. Xu, G. Brambilla, J. Feng, and Y. Lu, *IEEE Photon. Technol. Lett.* **22**, 218 (2010).
4. H. Yi, Y. Zhu, and Z. Zhou, *Chin. Opt. Lett.* **7**, 312 (2009).
5. L. Zhang, F. Gu, J. Lou, X. Yin, and L. Tong, *Opt. Express* **16**, 13349 (2008).
6. H. Zhu, Y. Wang, and B. Li, *ACS Nano* **3**, 3110 (2009).
7. Y. Wu, Y. Rao, Y. Chen, and Y. Gong, *Opt. Express* **17**, 18142 (2009).
8. M. Tonzzer and R. G. Lacerda, *Sensor Actuat. B Chem.* **150**, 517 (2010).
9. M. Belal, Z. Song, Y. Jung, G. Brambilla, and T. P. Newson, *Opt. Lett.* **35**, 3045 (2010).
10. A. Iadicicco, A. Cusano, A. Cutolo, R. Bernini, and M. Giordano, *IEEE Photon. Technol. Lett.* **16**, 1149 (2004).
11. B. Lin, S. C. Tjin, G. Wang, and P. Shum, *Phys. Procedia.* **19**, 315 (2011).
12. J. Kou, M. Ding, J. Feng, Y. Lu, F. Xu, and G. Brambilla, *Sensors* **12**, 8861 (2012).
13. X. Fang, C. Liao, and D. Wang, *Opt. Lett.* **35**, 1007 (2010).
14. H. Xuan, W. Jin, and M. Zhang, *Opt. Express* **17**, 21882 (2009).
15. M. Ding, M. N. Zervas, and G. Brambilla, *Opt. Express* **19**, 15621 (2011).
16. Y. Liu, C. Meng, A. P. Zhang, Y. Xiao, H. Yu, and L. Tong, *Opt. Lett.* **36**, 3115 (2011).
17. W. Luo, J. Kou, Y. Chen, F. Xu, and Y. Lu, *Appl. Phys. Lett.* **101**, 133502 (2012).
18. J. Kou, S. Qiu, F. Xu, and Y. Lu, *Opt. Express* **19**, 18452 (2011).
19. Y. Ran, Y. Tan, L. Sun, S. Gao, J. Li, L. Jin, and B. Guan, *Opt. Express* **19**, 18577 (2011).
20. Y. Ran, L. Jin, Y. Tan, L. Sun, J. Li, and B. Guan, *IEEE Photon. J.* **4**, 180 (2012).
21. J. Canning, *J. Sens.* **2009**, 871580 (2009).
22. Y. Zhang, B. Lin, S. C. Tjin, H. Zhang, G. Wang, P. Shum, and X. Zhang, *Opt. Express* **18**, 26345 (2010).
23. A. Yariv, *IEEE J. Quantum Electron.* **QE-9**, 919 (1973).
24. Y. Jung, G. Brambilla, and D. J. Richardson, *Opt. Express* **16**, 14661 (2008).
25. A. W. Snyder and J. D. Love, *Optical Waveguide Theory* (Chapman and Hall, New York, 1983).
26. T. A. Birks and Y. W. Li, *J. Lightwave Technol.* **10**, 432 (1992).
27. Y. Chen and Z. Ma, *Experiment Science and Technology* **6**, 16 (2010).